Gümüşhane University Journal of Science

GUFBD / *GUJS* (2023) 13(2): 458-470 doi: 10.17714/gumusfenbil.1122225 Research Article

# Estimation of Contact Lengths Using Deep Neural Network

## *Derin Öğrenme Yöntemi ile Temas Uzunlukları Tahmini*

**Alper POLAT** *1

[1]*Munzur University, Construction Technology Department, Tunceli, Turkey*

• Received: 27.05.2022 • Accepted: 24.03.2023

**Abstract**

One of the most common problems in engineering is contact problems. In recent years, researchers have turned to alternative methods that can offer effective solutions in a shorter time, instead of solutions containing complex and long mathematical expressions. This study focuses on the estimation of the contact lengths in a homogeneous elastic layer suppressed by two elastic punches with two solution methods. Firstly, a new model was designed for estimation using Deep Learning Neural Network (DNN), one of the deep learning structures. Estimation of contact lengths was provided with the output of the DNN model, which was fed with the homogeneous elastic layer, the ratio of shear modules of the punches and the input parameters of punch radii. The finite element method was used as the second solution method. The problem was modelled in the ANSYS programme, and the solution was made with the same parameters used in DNN modelled. The results obtained from both solutions were compared with the solutions obtained by the theory of elasticity and classical NN in the literature. It had been seen that the results obtained with DNN and ANSYS were compatible with the results obtained with analytical and classical NN and the margin of error was smaller.

**Keywords:** Contact problem; Deep learning neural network; Finite element method; Machine learning

***Öz***

*Mühendislikte yaygın olarak karşılaşılan problemlerden biri de temas problemleridir. Son yıllarda araştırmacılar karmaşık ve uzun matematiksel ifadeler içeren çözümler yerine daha kısa sürede etkili çözümler sunabilen alternatif yöntemlere yönelmişlerdir . Bu çalışmada, elastik iki dairesel punch ile bastırılan homojen elastik tabakada meydana gelen temas uzunluklarının tahmini yapılmıştır. Bu amaçla makine öğrenmesi alanında son zamanların popüler konusu olan derin öğrenme tekniği kullanılmıştır. Derin öğrenme yapılarından Derin Öğrenme Sinir Ağı (DNN) kullanılarak tahmin için yeni bir model tasarlanmıştır. Homojen elastik tabaka ile punchların kayma modülleri oranı ve punch yarıçaplarından oluşan giriş parametreleri ile beslenen DNN modelinin çıkışında temas uzunluklarının tahmini sağlanmıştır. Modelin eğitimi için analitik çözüm ile elde edilen veriler kullanılmıştır. Ayrıca, sonlu elemanlar yöntemi ile çözümden elde edilen sonuçlar sunulmuş ve DNN sonuçları desteklenmiştir. Çalışmada elde edilen sonuçlar, literatürdeki elastisite teorisi ve klasik Neural Network ile yapılan çözümlerden elde edilen sonuçlarla kıyaslanmıştır. Sonuç olarak klasik Neural Network ile yapılan çözüme kıyasla DNN modeli çok daha kısa sürede ve daha az hatayla sonuçlar elde etmiştir. Sunulan bu modelin temas uzunluğu tahmininde kullanılabilecek etkili bir yaklaşım olduğu söylenebilir.*

***Anahtar kelimeler**: Temas roblemi; derin öğrenme; sonlu elemanlar yöntemi; makine öğrenmesi*

* Alper POLAT; alperpolat@munzur.edu.tr

ISSN: 2146-538X e-ISSN: 2146-538X https://dergipark.org.tr/tr/pub/gumusfenbil

## 1. Introduction

Contact problems are a common field of study for researchers in mechanical engineering. In engineering structures, many systems need to be in contact with each other to work. It is crucial for engineers to know the stresses, strains and displacements that result from the contact interaction of these systems. Data such as stress, strain and contact lengths of the systems provide great convenience during the design and sizing phase in contact problems. Starting with (Hertz, 1985) this phenomenon has led to interesting studies in a wide variety of materials and geometries Some of these studies have been on split contact problems (Kahya et al. 2007), (Rhimi et al. 2011), (El Borgi et al. 2017).

Studies on layer weights focus on the problems of continuous contact and discontinuous contact. If the load on the layer is below a certain limit, no separation occurs and this is called continuous contact. Researchers have conducted different studies by ignoring, as well as not ignoring, the friction effect (Chidlow et al. 2013), (Yan & Me, 2017), (Liu et al. 2018), (Polat et al. 2018). Contribution to the problems of contact problems has also been made with alternative solution methods. The finite element method has been one of the most preferred methods in these studies (Abhilash&Murthy, 2014), (Polat et al. 2019), Yaylacı (2017), (Alinia et al. 2018).

When the studies are examined, it can be seen that the theory of elasticity and computer-based numerical methods are preferred for the solution of contact problems. Some researchers have found the learning ability of machines beneficial. Through artificial neural networks (ANN), one of these methods, solutions have been developed for contact problems. (Özşahin et al. 2004) gathered ANN with the problem of contact in the homogeneous layer suppressed by two rigid blocks. An ANN model was applied by (Rapetto et al. 2009) for the determination of the relationship between unevenness parameters and real contact area. Khaleghian et al. made estimations on the friction values between tire and road using ANN (Khaleghian et al.2016). (Çakıroğlu et al. 2011) made the estimation of the contact distances in the elastic layer which is situated on two elastic quarter planes and pressed with a circular rigid punch by using ANN. In the study, they used a network structure with a three-layered backpropagation training algorithm.

Deep learning neural networks, which have recently been widely used in machine learning, are multi-layered structures of traditional ANN (Lecun et al. 2015). Advances in hardware and improvements in software approaches such as activation functions and optimizer have enabled the use of multi-layered networks. Common networks such as Convolutional Neural Networks (CNN), Stacked Autoencoders (SAE), Long Short-Term Memory (LSTM) provide very successful results in deep learning. CNNs are particularly popular in image processing (Krizhevsky et al. 2015), (Çelik et al. 2020). It can perform classification with an end-to-end architecture without the need for any manual feature extraction on image data (Goodfellow et al. 2016). Besides the two-dimensional input data, notable results were obtained within the 1D input data. These structures are frequently used especially in the biomedical signal processing field (Murat et al. 2020), (Yıldırım et al. 2018). On account of multi-layer structures, high performance has been achieved in areas such as image processing, sound processing and signal processing, with features abstracted in deep layers. On the other hand, DNNs are multi-layered structures of classical neural network architecture. These networks offer successful applications in classification and regression problems.

In this study, the estimation of contact lengths in a homogeneous and isotropic layer suppressed by two elastic circular punches was obtained through Deep Learning Neural Network (DNN). It was aimed to automatically estimate contact lengths at the output using the input parameters of the DNN networks. For this purpose, the design of the network that would provide the best result was done by determining the optimum DNN layer parameters. Reducing the use of hardware resources and obtaining the best results were taken into consideration while creating the DNN. The finite element method was used as a second solution. The problem was modeled with ANSYS Mechanical Launcher to obtain contact lengths. The results from both solutions were compared with those obtained by (Özşahin et al. 2004) using the theory of elasticity and ANN.

## 2. Definition of the problem

### 2.1. Geometry of the problem and boundary conditions

The geometry of the homogeneous and isotropic layer in the range (-∞, +∞) suppressed by two elastic circular punch was presented in Figure 1. The material properties of the elastic layer were given as ($\mu_1$, $\upsilon_1$). The material properties for circular punches were defined as ($\mu_2$, $\upsilon_2$) and ($\mu_3$, $\upsilon_3$), respectively. Here, μ represents the shear modulus. In the problem, friction effects were neglected and the punches were accepted to transfer compressive stresses only.

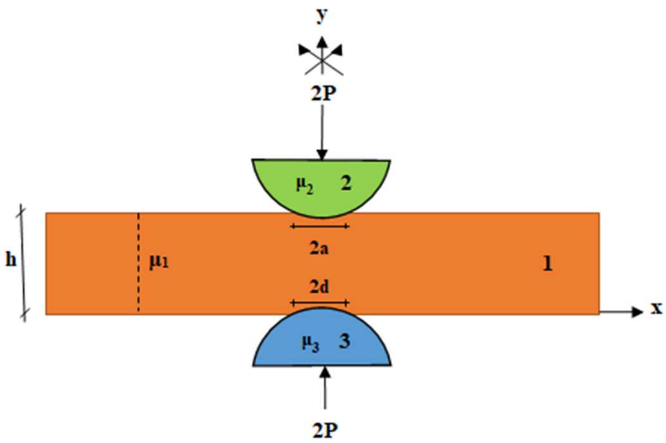


**Figure 1.** Geometry of the problem

The general equations belonging to stresses and displacements in case of neglection of body forces in the FG layer were obtained using the theory of Elasticity and Fourier integral transformation technique. Expressions for the linear elastic stress-displacement situation are as follows:

The boundary conditions for the problem are as follows.

$$\tau_{xy_1}(x,0)=0 \qquad 0\le x<\infty \tag{1}$$

$$\tau_{xy_2}(x,0)=0 \qquad 0\le x<\infty \tag{2}$$

$$\tau_{xy_1}(x,h)=0 \qquad 0\le x<\infty \tag{3}$$

$$\tau_{xy_3}(x,h)=0 \qquad 0\le x<\infty \tag{4}$$

$$\sigma_{y_1}(x,h)=-\omega_1(x) \qquad 0\le x<a \tag{5}$$

$$\sigma_{y_1}(x,0)=-\omega_2(x) \qquad 0\le x<d \tag{6}$$

$$\sigma_{y_1}(x,0)=\sigma_{y_2}(x,0) \qquad 0\le x<\infty \tag{7}$$

$$\sigma_{y_1}(x,h)=\sigma_{y_3}(x,h) \qquad 0\le x<\infty \tag{8}$$

$$\frac{\partial\left[v_1(x,h)-v_3(x,h)\right]}{\partial x}=\zeta_1(x) \qquad 0\le x<a \tag{9}$$

$$\frac{\partial\left[v_1(x,h)-v_2(x,h)\right]}{\partial x}=\zeta_2(x) \qquad 0\le x<d \tag{10}$$

Since the geometry was symmetrical, $a$ and $d$ were taken as half contact lengths. $\zeta_1(x)$ and $\zeta_2(x)$ were unknown contact stresses. This function was taken as follows:

$$\zeta_1(x)=x\left(\Gamma_1^2-x^2\right)^{-\frac{1}{2}} \tag{11}$$

$$\zeta_2(x) = -x\left(\Gamma_2^2 - x^2\right)^{-\frac{1}{2}} \quad (12)$$

$\Gamma_1$ ve $\Gamma_2$ in these functions were the radii of the elastic circular punches.

### 2.2. Contact dataset

As the dataset in the study, 400 contact length data obtained from the theory of elasticity solution by (Özşahin et al. 2004) based on the theory of elasticity with various materials and loading conditions were used as input parameters. Parameters and value ranges in the dataset were given in Table 1. The values of $\mu_2/\mu_1$ and $\mu_3/\mu_1$ in this table represent the lower punch shear modulus-homogeneous layer shear modulus ratio and the upper punch shear modulus-homogeneous layer shear modulus ratio, respectively. These values were obtained in-between 0.52, 1.65, 2.8 and 5 in various variations.

**Table 1.** Material properties and loading status used in the dataset

| *Parameters* | *Representation* | *Value interval* |
|---|---|---|
| Ratio of shear modulus of lower elastic punch to elastic layer | $\mu_2/\mu_1$ | 0.52-5 |
| Ratio of shear modulus of lower elastic punch to elastic layer | $\mu_3/\mu_1$ | 0.52-5 |
| Ratio of radius of upper elastic layer height | $\Gamma_1/h$ | 10, 100, 1000 |
| Ratio of radius of lower elastic layer height | $\Gamma_2/h$ | 10, 100, 1000 |
| Load factor | $\mu_1 h/P$ | 100-1500 |

### 2.3. Deep Learning Neural Networks

Information about the materials and methods used in the study was given in this section. The contact length data obtained in the study and the characteristics of the data were mentioned. Detailed information about the DNN model used for predictions was presented. A general representation of the method used in the study was given in Figure 2.

The deep learning approach can simply be considered as multi-layered structures of classical NN architectures. Deep multi-layered structures have many nonlinear levels and they can represent a highly nonlinear and diverse range of functions compactly with these structures (Bengio et al. 2007). Hence, they can be more efficient learning structures in terms of representation. In 2006, the birth of deep learning techniques happened with a new training method introduced by Hinton et al. (Hinton et al. 2006). With the success on ImageNet (Krizhevsky et al. 2015) image data, deep learning became the most popular subject of machine learning. An illustration representing the functioning of a neuron in a classic NN structure was given in Figure 3 to show how DNN structures work.

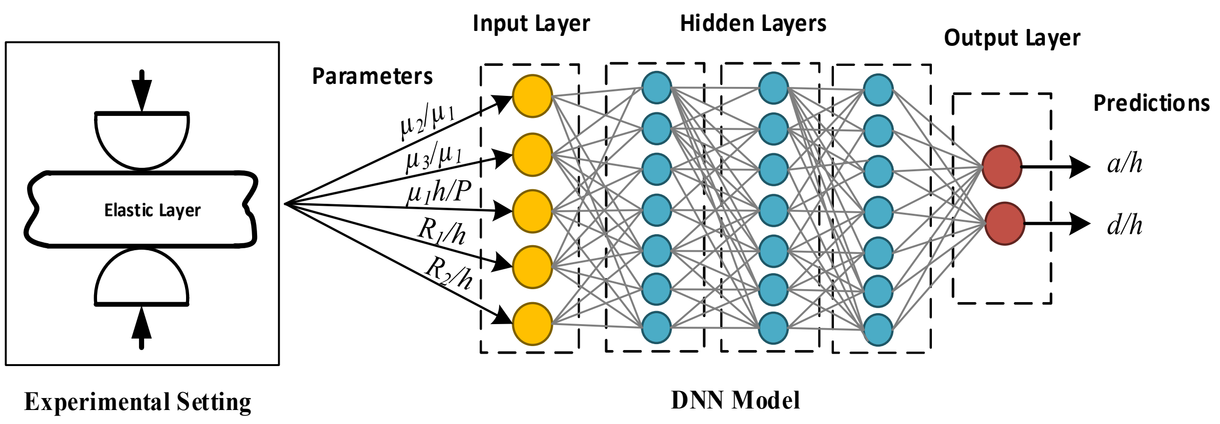


**Figure 2.** A general representation of DNN method for this study

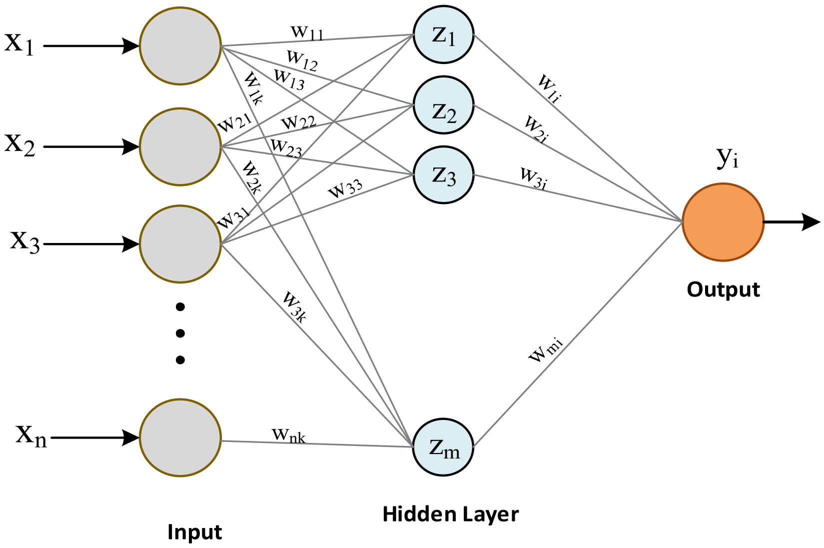


**Figure 3.** Structures of the classic neural network

The output value calculation for each hidden layer neuron with weights as w and x input was shown in Eq.(13).

$$z_j = f(\sum_{i=1}^{N} w_{ij} x_i + b_j) \tag{13}$$

Each hidden layer output was similarly multiplied by its weight values and passed through an activation function to obtain the neuron output in Eq.(14).

$$y_i = \sigma(\sum_{j=1}^{M} w_{ji} z_j + b_j) \tag{14}$$

A conversion operation that would the input data to the output data was performed utilizing the σ activation function. It also played an active role in solving complex problems with its nonlinear characteristic. Calculation of the Rectified Linear Unit (ReLU) activation function commonly used in DNNs was given in Eq. (15).

$$f(x) = \begin{cases} 0, & \text{if } x < 0 \\ x, & \text{if } x \geq 0 \end{cases} \tag{15}$$

A block representation representing the difference between classic NN networks and DNN networks was given in Figure 4.

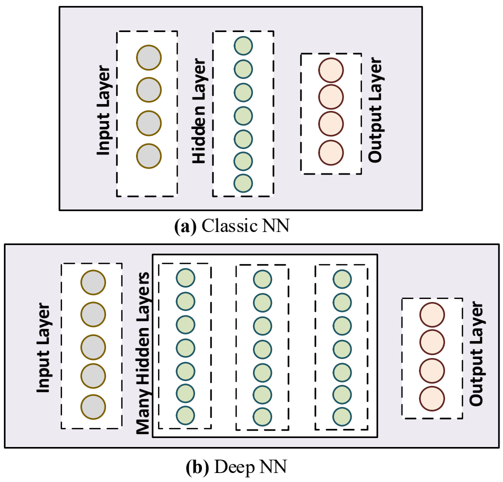


**Figure 4.** Structures of the classic NN (a) and deep NN (b)

### 2.3.1. The Proposed DNN Model

This study's purpose was to automatically estimate contact lengths (a/h and d/h) at the output using the input parameters of the DNN networks. For this purpose, the design of the network that would provide the best result was done by determining the optimum DNN layer parameters. Reducing the use of hardware resources and obtaining the best results were taken into consideration while creating the DNN. Layer parameters and layer numbers were adjusted by trial and error approach while creating DNN layers. The block representation of the 8-layer DNN structure designed in the study was given in Figure 5.

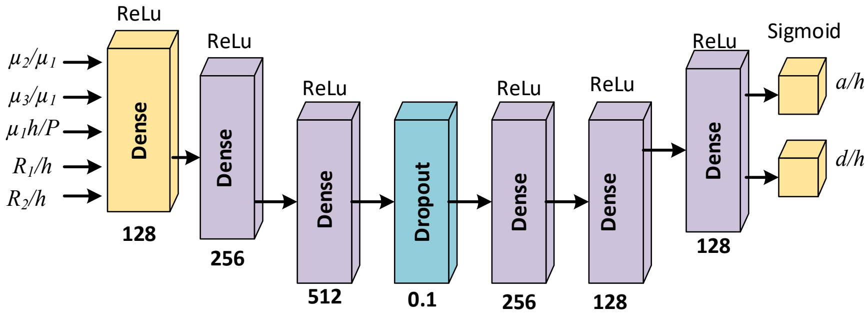


**Figure 5.** Block diagram representation of the DNN model used

The input of the DNN network consists of the following parameters.

$\mu_2/\mu_1$: Ratio of shear modulus of lower elastic punch to elastic Layer
$\mu_3/\mu_1$: Ratio of shear modulus of lower elastic punch to elastic Layer
$\mu_1 h/P$: Load factor
$\Gamma_1/h$: Ratio of radius of upper elastic layer height
$\Gamma_2/h$: Ratio of radius of lower elastic layer height

There were hidden layers with 128, 256 and 512 units and a layer with 0.1 dropout ratio in the DNN network. The activation function of hidden layers was chosen as the Rectified Linear Unit (ReLU), which is widely used in the deep learning field. The last layer of the DNN network was the output layer, and it contains two neurons. Sigmoid was chosen as the activation function. As a result of the training of the deep network, dimensionless contact lengths (a/h ve d/h) were estimated at the output using the input parameters. Some hyperparameter adjustments used during the training of the model were shown in Table 2.

**Table 2.** Some hyperparameters and values of the proposed model

| Hyper parameters | Value |
|---|---|
| Optimizer | Adam |
| Learning rate | 0.001 |
| Decay | 0.001 |
| Batch Size | 32 |
| Number of epochs | 200 |
| Loss function | Mean Squared Logaritmic Error (MSLE) |

### 2.4. FEM process

The finite element method (FEM) is a widely used method in engineering, especially in the analysis and sizing phase. The main feature of this method is to find a solution to a complex problem by replacing it with a simpler method. It addresses the solution region that consists of many smaller and interconnected sub-regions called finite elements. In each piece or element, a suitable approximate solution is assumed and general equilibrium conditions are created. This method has been used successfully in the solution of various engineering problems such as heat conduction, fluid dynamics, leakage flow and electromagnetic fields, as well as being widely used structural mechanics field. Researchers have recently preferred fast and effective computer programs based on the FEM solution principle. One of them is the ANSYS Mechanical APDL Product Launcher program, which is also used in this study. Because the study is a static and 2D plane problem, 8-node PLANE183 is used as the element type. This element does not have complete rotation freedom but has a degree of freedom in both the x and y directions. Geometry was divided into finite networks with free triangular mesh. CONTA172 and TARGE169 surface elements were chosen as contact pairs. ANSYS model of the problem was presented in Figure 6.

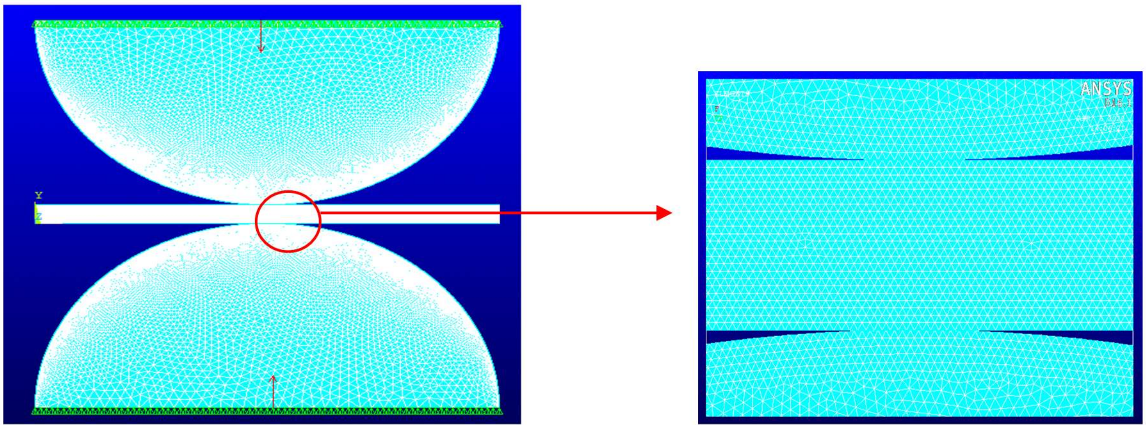


**Figure 6.** ANSYS model of the problem

## 3. Results and discussions

### 3.1. DNN results

In the experimental studies of the model, 400 contact length data obtained with different parameters were used making use of the theory of elasticity. The data were divided as 80%, 20% and 10%, as training, validation and testing, respectively. The test data were those that the model does not see during the training phase, after which it produces estimates. All parameters were normalized to 0-1 range as pre-processing on the input data. The loss graphs in the training stage of DNN and NN models with a single hidden layer were given in Figure 7.

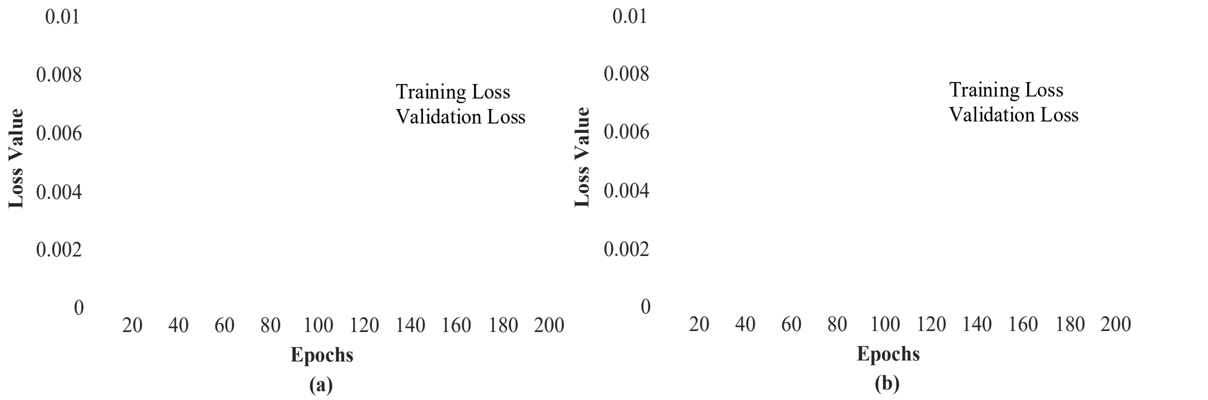


**Figure 7**. Loss plots of models over 500 epoch a) DNN model b) NN model with a single hidden layer

Figure 7(a) demonstrated that the DNN model has reached a loss value of 0.0003 in approximately 20 epochs. Meanwhile, this value could decrease to 0.003 levels if a traditional neural network with a hidden layer of 128 units was used instead of the deep model, which was shown in Figure 7(b). These results showed the effect of deepening the layers on training. Also, there was a significant difference between these values in the NN network while the training loss (blue lines) and validation loss (orange lines) in the DNN network were very close to each other. This was an important parameter that showed that the training phase of the network was validated on the validation datasets. The graphical representation of the contact length estimates made by the DNN model on the test data after its training was shown in Figure 8.

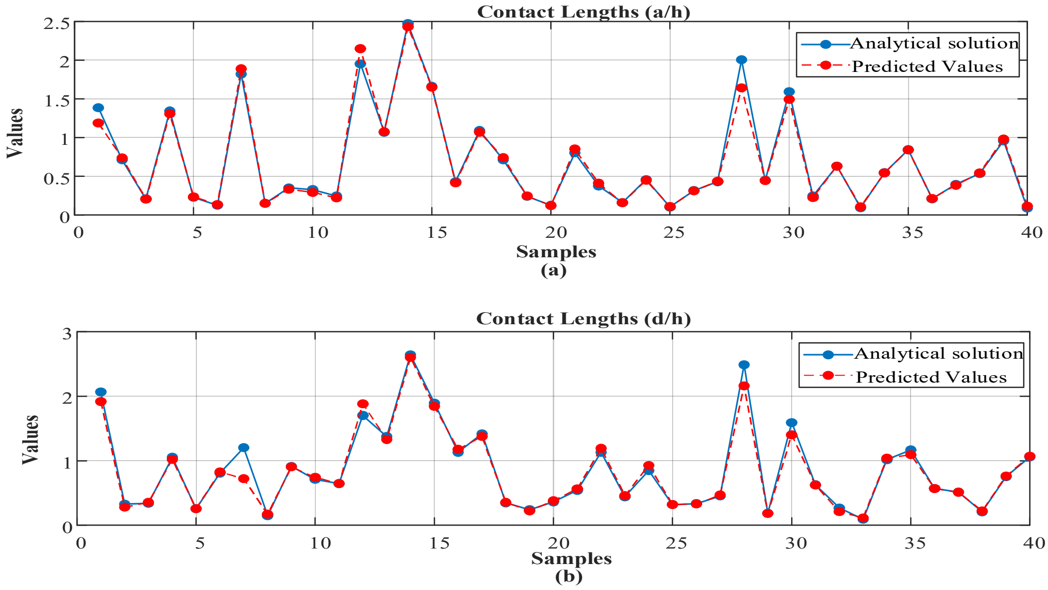


**Figure 8**. The comparison of the contact lengths estimates made by the DNN model for the test data. a) Output parameter (a / h), b) Output parameter (d / h)

These results showed that the model estimates matched the actual values rather well. 40 test input data and the numerical values of the estimates obtained by the DNN model for these data were given in Table 3. Besides, a comparison between the input parameters and the actual parameter values that were obtained was made. These comparisons were DNN and FEM solutions given in this study with analytical and NN results by (Özşahin et al. 2004).

**Table 3.** DNN Model Predicted Results

| **Input parameters** | | | | | **Analytical outputs** | | **Predicted outputs** | |
|---|---|---|---|---|---|---|---|---|
| $\mu_2/\mu_1$ | $\mu_3/\mu_1$ | $\Gamma_1/h$ | $\Gamma_2/h$ | $\mu_1 h/P$ | *a/h* | *d/h* | *a/h* | *d/h* |
| 0.52 | 5 | 100 | 1000 | 100 | 1.3846 | 2.0675 | 1.1886 | 1.9200 |
| 5 | 5 | 1000 | 100 | 1000 | 0.7109 | 0.3266 | 0.7366 | 0.2796 |
| 0.52 | 5 | 10 | 10 | 250 | 0.2071 | 0.3397 | 0.2048 | 0.3545 |
| 12.8 | 5 | 1000 | 100 | 100 | 1.3425 | 1.0550 | 1.3078 | 1.0209 |
| 1.65 | 5 | 10 | 10 | 250 | 0.2267 | 0.2554 | 0.2329 | 0.2580 |
| 1.65 | 1.65 | 10 | 1000 | 1000 | 0.1238 | 0.8094 | 0.1353 | 0.8265 |
| 0.52 | 0.52 | 1000 | 100 | 250 | 1.8215 | 1.2027 | 1.8891 | 0.7224 |
| 5 | 5 | 10 | 10 | 500 | 0.1480 | 0.1480 | 0.1480 | 0.1696 |
| 0.52 | 0.52 | 10 | 100 | 250 | 0.3497 | 0.9127 | 0.3303 | 0.9047 |
| 5 | 5 | 100 | 1000 | 1000 | 0.3267 | 0.7109 | 0.2916 | 0.7410 |
| 1.65 | 2.8 | 10 | 100 | 250 | 0.2438 | 0.6451 | 0.2185 | 0.6479 |
| 0.52 | 1.65 | 1000 | 100 | 100 | 1.9540 | 1.7031 | 2.1491 | 1.8826 |
| 0.52 | 5 | 1000 | 1000 | 1000 | 1.0684 | 1.3774 | 1.0745 | 1.3303 |
| 0.52 | 2.8 | 1000 | 1000 | 250 | 2.4724 | 2.6442 | 2.4329 | 2.6036 |
| 0.52 | 2.8 | 1000 | 1000 | 500 | 1.6609 | 1.8937 | 1.6520 | 1.8447 |
| 0.52 | 1.65 | 100 | 1000 | 1000 | 0.4272 | 1.1302 | 0.4152 | 1.1773 |
| 2.8 | 2.8 | 100 | 1000 | 100 | 1.0907 | 1.4190 | 1.0697 | 1.3771 |
| 2.8 | 5 | 100 | 10 | 100 | 0.7129 | 0.3478 | 0.7395 | 0.3540 |
| 1.65 | 1.65 | 10 | 10 | 250 | 0.2399 | 0.2399 | 0.2446 | 0.2236 |
| 1.65 | 1.65 | 10 | 100 | 1000 | 0.123 | 0.3616 | 0.1197 | 0.3790 |
| 0.52 | 2.8 | 100 | 10 | 100 | 0.8025 | 0.5399 | 0.8523 | 0.5653 |
| 1.65 | 5 | 10 | 1000 | 100 | 0.3735 | 1.1307 | 0.4095 | 1.1940 |

**Table 3.** DNN Model Predicted Results (Continue)

| | | | | | | | | |
|---|---|---|---|---|---|---|---|---|
| 2.8 | 2.8 | 10 | 100 | 500 | 0.1585 | 0.4414 | 0.1570 | 0.4575 |
| 5 | 5 | 100 | 1000 | 500 | 0.4576 | 0.8487 | 0.4464 | 0.9286 |
| 1.65 | 2.8 | 10 | 100 | 1500 | 0.1007 | 0.3204 | 0.1082 | 0.3224 |
| 2.8 | 5 | 100 | 100 | 1000 | 0.3151 | 0.3350 | 0.3110 | 0.3291 |
| 2.8 | 5 | 100 | 100 | 500 | 0.4287 | 0.4551 | 0.4341 | 0.4696 |
| 0.52 | 0.52 | 100 | 1000 | 100 | 2.0058 | 2.4900 | 1.6413 | 2.1627 |
| 1.65 | 5 | 100 | 10 | 500 | 0.4462 | 0.1851 | 0.4449 | 0.1825 |
| 0.52 | 0.52 | 100 | 100 | 100 | 1.5917 | 1.5917 | 1.4938 | 1.4020 |
| 1.65 | 1.65 | 10 | 100 | 250 | 0.244 | 0.6264 | 0.2239 | 0.6213 |
| 5 | 5 | 1000 | 100 | 1500 | 0.6298 | 0.2682 | 0.6305 | 0.2098 |
| 2.8 | 2.8 | 10 | 10 | 1500 | 0.092 | 0.0920 | 0.1040 | 0.1149 |
| 1.65 | 1.65 | 100 | 1000 | 500 | 0.5448 | 1.0160 | 0.5427 | 1.0402 |
| 0.52 | 5 | 1000 | 1000 | 1500 | 0.8424 | 1.1678 | 0.8392 | 1.0942 |
| 2.8 | 5 | 10 | 100 | 250 | 0.2093 | 0.5698 | 0.2118 | 0.5692 |
| 0.52 | 1.65 | 10 | 10 | 100 | 0.3946 | 0.5130 | 0.3836 | 0.5120 |
| 5 | 5 | 100 | 10 | 250 | 0.5341 | 0.2089 | 0.5426 | 0.2223 |
| 0.52 | 5 | 1000 | 100 | 500 | 0.956 | 0.7531 | 0.9808 | 0.7647 |
| 0.52 | 5 | 10 | 1000 | 1500 | 0.0871 | 1.0599 | 0.1135 | 1.0699 |

### 3.2. FEM results

The ANSYS model of a homogeneous elastic layer pressed with two rigid punches is given in Figure 9. The contact stress analysis of the materials according to the shear modules and loading conditions and the contact lengths between the punches and the sheet were examined. The contact distance after the analysis was visually presented in Figure 10. The effect of different shear modules on the contact stress with punches pressed under equal loads was investigated. The dimensionless d/h distance graph was presented in Figure 11 after the ANSYS analysis of the problem, about which the loading and material properties were given. It can be seen that the values found also matched the table values.

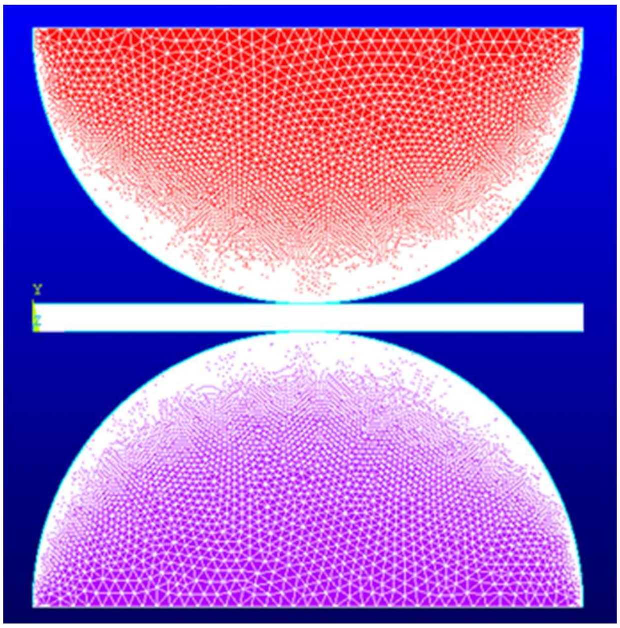

**Figure 9.** ANSYS model of homogeneous layer loaded by two elastic punch

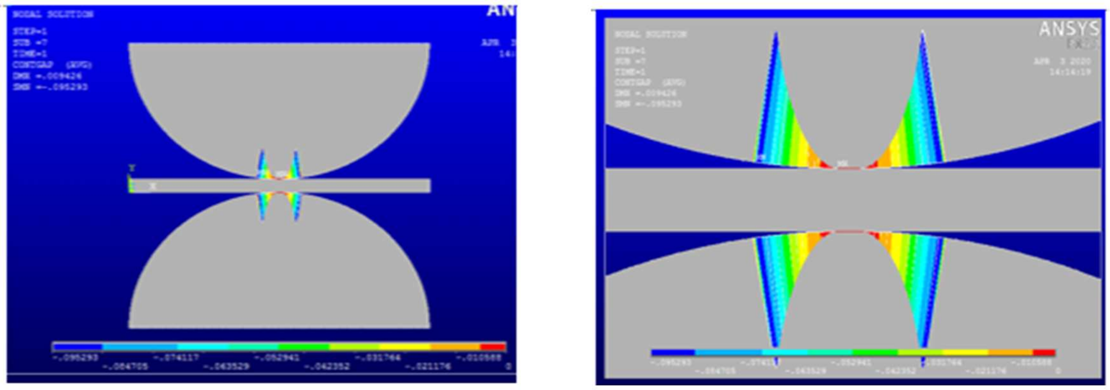


**Figure 10.** Contact Gap Distance ($\mu_2/\mu_1$=1.65, $\mu_3/\mu_1$=2.8, $\Gamma_1$/h=10, $\Gamma_2$/h=10, $\mu_1$h/P=250). a) Contact Gap Distance, b) Zoom Model

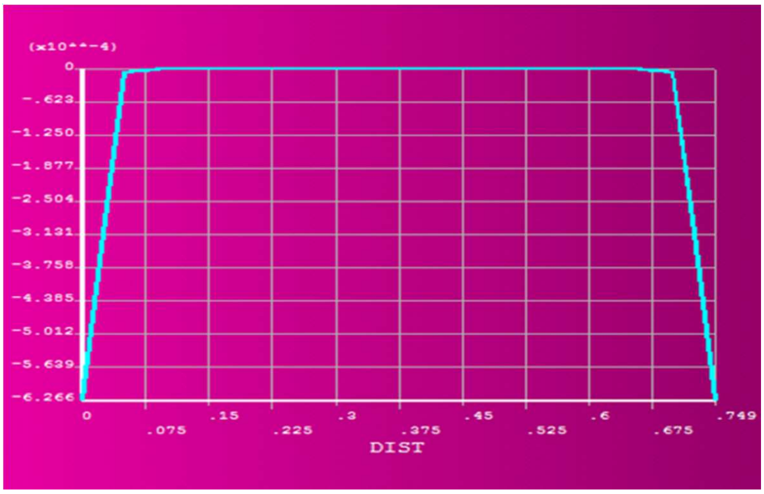


**Figure 11.** Contact length of second punch (d/h=0.61 ) ($\mu_2/\mu_1$=1.65, $\mu_3/\mu_1$=5, $\Gamma_1$/h=100, $\Gamma_2$/h=100, $\mu_1$h/P=350)

### 3.3. Comparison of the results

In this section, DNN and FEM results obtained in the study were presented comparatively with tables and figures. Contact lengths obtained according to different material properties for elastic punches with the same radii were given in Table 4. It was seen that the results of DNN and FEM were compatible with the results of the study conducted in the previous studies based on the theory of elasticity. Figure 12 graphically supported these results.

**Table 4.** Comparison of contact lengths according to different material parameters ($\Gamma_1$/h=10, $\Gamma_2$/h=10)

| *Material Properties* | | | *Analytical Solution* | | *DNN* | | *FEM* | |
|---|---|---|---|---|---|---|---|---|
| $\mu_2/\mu_1$ | $\mu_3/\mu_1$ | $\mu_1 h/P$ | *a/h* | *d/h* | *a/h* | *d/h* | *a/h* | *d/h* |
| 0.52 | 1.65 | 1500 | 0.1081 | 0.1405 | 0.1091 | 0.1471 | 0.105 | 0.140 |
| 0.52 | 5 | 100 | 0.3210 | 0.5186 | 0.3116 | 0.5041 | 0.315 | 0.505 |
| 1.65 | 2.8 | 250 | 0.2387 | 0.2556 | 0.2497 | 0.2066 | 0.225 | 0.248 |
| 1.65 | 5 | 500 | 0.1631 | 0.1840 | 0.1572 | 0.1851 | 0.161 | 0.185 |
| 2.8 | 5 | 1000 | 0.1055 | 0.1124 | 0.1191 | 0.1311 | 0.104 | 0.110 |

The comparative data of the results obtained with DNN and FEM, with the theory of elasticity and the solution with the classical NN method were shown in Table 5 and Figure 13. Contact lengths found in the analysis using the load factor values between 150-1250 were found to be compatible with acceptable error rates.

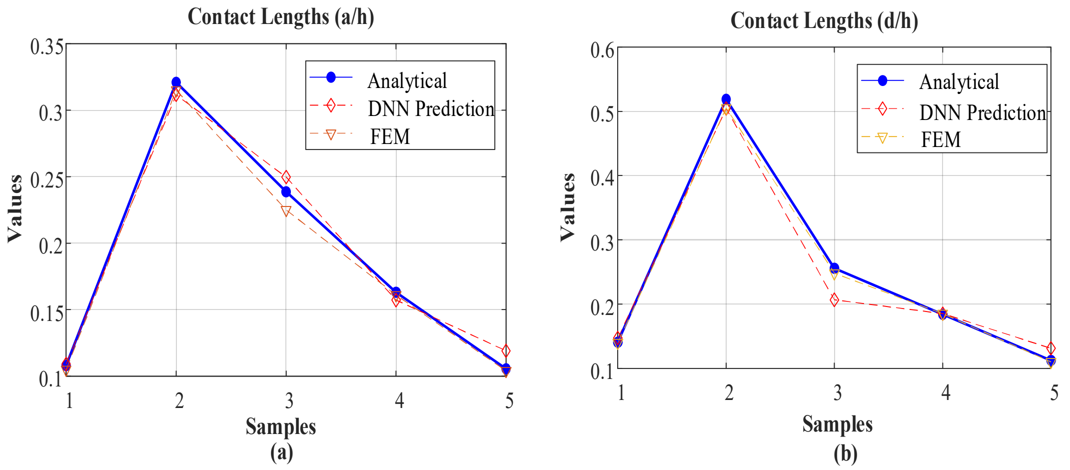


**Figure 12.** Comparative graph of contact lengths obtained with different solution methods

**Table 5.** Comparison of contact lengths obtained according to all solution methods ($\mu_2/\mu_1$=1.6, $\mu_3/\mu_1$=5, $\Gamma_1$/h=100, $\Gamma_2$/h=100)

| $\mu_1 h/P$ | *a/h* | | | | *d/h* | | | |
|---|---|---|---|---|---|---|---|---|
| | *Özşahin et al. [19]* | | *Proposed study* | | *Özşahin et al. [19]* | | *Proposed study* | |
| | *Analytical* | *NN* | *DNN* | *FEM* | *Analytical* | *NN* | *DNN* | *FEM* |
| 150 | 0.7947 | 0.7831 | 0.8188 | 0.785 | 0.8646 | 0.8815 | 0.8643 | 0.875 |
| 350 | 0.5481 | 0.5280 | 0.5421 | 0.540 | 0.6089 | 0.6159 | 0.5922 | 0.610 |
| 450 | 0.4912 | 0.4757 | 0.4836 | 0.490 | 0.5476 | 0.5560 | 0.5346 | 0.545 |
| 650 | 0.4178 | 0.4069 | 0.3971 | 0.410 | 0.4680 | 0.4729 | 0.4578 | 0.465 |
| 750 | 0.3911 | 0.3818 | 0.3731 | 0.385 | 0.4399 | 0.4415 | 0.4281 | 0.410 |
| 1250 | 0.3119 | 0.3091 | 0.3053 | 0.305 | 0.3509 | 0.3451 | 0.3418 | 0.355 |

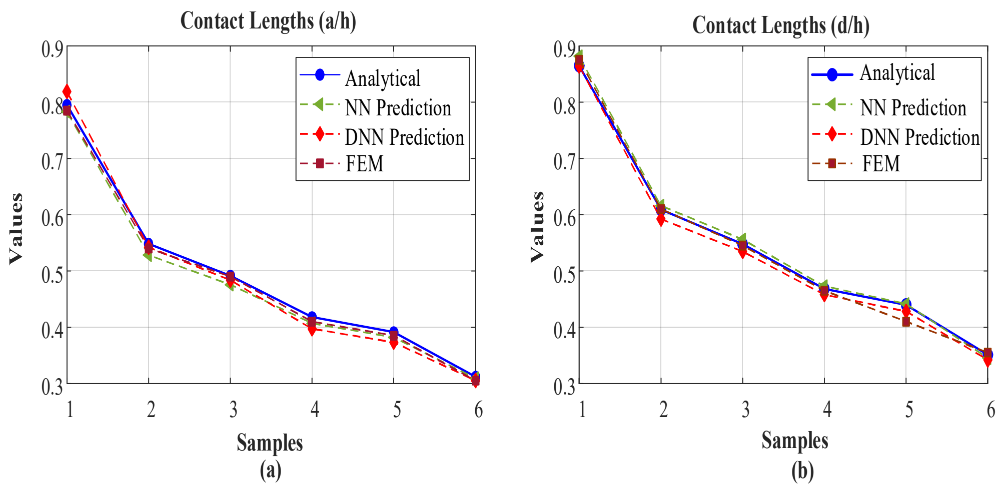


**Figure 13.** Comparative graph of contact lengths obtained with all solution methods

## 4. Conclusions

In this study, a new DNN model was proposed for estimation on the contact length problem. DNN model trained on the data obtained by analytical solutions was used to estimate the contact lengths with the input parameters. In the study, a comprehensive comparison between analytical solution, finite element solution, NN prediction and DNN was made for the contact problem. In the estimation study with NN networks, the results obtained with high epochs such as 50000 were obtained in only such a short time as 200 epochs with the DNN network. In addition, the estimation results of the DNN network had less error ratio than the classical NN compared to the solution made based on the theory of elasticity. The obtained results were supported by the solution made with the finite element method. The results obtained from this study showed that the analysis of contact problems with deep learning can be done easily and quickly. In the future, contact problems with functional graded or piezoelectric layers instead of elastic layers can also be solved.

**Acknowledgments**

I would like to say many thanks to Dr. Özal Yıldırım for contributing to my study.

**Author contribution**

Research design, finite elements calculations, data analysis, article writing and final approval.

**Declaration of ethical code**

The author of this article declares that the materials and methods used in this study do not require ethical committee approval and/or legal-specific permission.

**Conflicts of interest**

The author declares that there is no conflict of interest.

**References**

Abhilash, M.N., & Murthy, H. (2014). Finite element analysis of 2-D elastic contacts involving FGMs, *International Journal of Computer Methods Engineering Science Mechanic*, *15*(3), 253–7. https://doi.org/10.1080/15502287.2014.882445

Alinia Y., Aisaee, A. & Hosseini-Nasab, M. (2019). Stress analysis in rolling contact problem of a finite thickness FGM layer*, Meccanica, 54*, 183–203. https://doi.org/10.1007/s11012-018-00925-w

ANSYS. (2016). *Swanson Analysis Systems Inc.*, Houston PA, USA.

Bengio Y., Lamblin P., Popovici D. & Larochelle H. (2006). Greedy layer-wise training of deep networks, *In Advances in Neural Information Processing Systems, 19*, 153-160.

Chidlow S.J., Chong W.W.F. & Teodorescu M. (2013). On the two-dimensional solution of both adhesive and non-adhesive contactproblems involving functionally graded materials, *European Journal of Mechanics A/Solids. 39*, 86–103. https://doi.org/10.1016/j.euromechsol.2012.10.008

Çakiroğlu E., Çömez I. & Erdöl R. (2011). İki elastik çeyrek düzleme oturan ve dairesel rijit bir punch ile bastırılan elastik tabaka probleminde temas mesafelerinin yapay sinir ağı ile hesabı, *VII. Ulusal Mekanik Kongresi* (pp. 192-201), Elazığ.

Çelik Y., Talo, M., Yildirim Ö., Karabatak M. & Acharya U.R. (2020). Automated invasive ductal carcinoma detection based using deep transfer learning with whole-slide images, *Pattern Recognition Letters, 133*, 232-239. https://doi.org/10.1016/j.patrec.2020.03.011

El-Borgi S. & Çömez I. (2017). A receding frictional contact problem between a graded layer and a homogeneous substrate pressed by a rigid punch, *Mechanics of Materials, 114*, 201-214. https://doi.org/10.1016/j.mechmat.2017.08.003

Goodfellow I., Bengio Y. & Courville A. (2016). *Deep learning,* T. Dietterich, Ed. London, England: The MIT Press.

Hinton G. E., Osindero S. & Teh Y. W. (2006). A fast learning algorithm for deep belief nets, *Neural Computation*. *18*(7), 1527-1554.

Johnson K.L. (1985). *Contact mechanics,* First Edition, Cambrigde University Press, Cambridge.

Kahya V., Özşahin T.Ş., Birinci A. & Erdöl R. (2007). A receding contact problem for an anisotropic elastic medium consisting of a layer and a half plane, *International Journal of Solids and Structures. 44,* 5695-5710.

Khaleghian S., Ghasemalizadeh O. & Taheri S. (2016). Estimation of the tire contact patch length and normal load using intelligent tires and its application in small ground robot to estimate the tire-road friction, *Tire Science and Technology. 44*(4), 248-261. https://doi.org/10.2346/tire.16.440402

Krizhevsky A., Sutskever I. & Hinton G.E. (2015). Imagenet classification with deep convolutional neural networks, *In Advances in Neural Information Processing Systems, 25*, 1097-1105.

Lecun Y., Bengio Y. & Hinton G. (2015). Deep learning, *Nature, 521*(7553), 436-444. https://doi.org/10.1038/nature14539

Liu Z., Yan J. & Mi C. (2018). On the receding contact between a two-layer inhomogeneous laminate and a half-plane, *Structural Engineering and Mechanics, 66*(3), 329-341. https://doi.org/10.12989/sem.2018.66.3.329

Murat F., Yildirim Ö., Talo M., Baloglu U.B., Demir Y. & Acharya U.R. (2020). Application of deep learning techniques for heartbeats detection using ECG signals-Analysis and Review, *Computers in Biology and Medicine, 120*,103726. https://doi.org/10.1016/j.compbiomed.2020.103726

Özşahin T.Ş., Birinci A. & Çakıroğlu A.O. (2004). Prediction of contact lengths between an elastic layer and two elastic punches with neural networks, *Structural Engineering and Mechanics, 18*(4), 441-459.

Polat A., Kaya Y. & Özsahin T.Ş. (2018). Analytical solution to continuous contact problem for a functionally graded layer loaded through two dissimilar rigid punches, *Meccanica, 53*(14), 3565-3577. https://doi.org/10.1007/s11012-018-0902-7

Polat, A. Kaya, Y. Kouider B. & Özşahin T.Ş. (2019). Frictionless contact problem for a functionally graded layer loaded through two rigid punches using finite element method, *Journal of Mechanics, 35*(5), 591-600. https://doi.org/10.1017/jmech.2018.55

Rapetto M.P., Almqvist A., Larsson R. & Lugta P.M. (2006). On the influence of surface roughness on real area of contact in normal, dry, friction free, rough contact by using a neural network, *Wear, 266*(5-6) 592-595.

Rhimi M., El-Borgi S. & Lajnef N. (2011). A double receding contact axisymmetric problem between a functionally graded layer and a homogeneous substrate, *Mechanics of Materials, 43*, 787–798. https://doi.org/10.1016/j.mechmat.2011.08.013

Yaylacı M. (2017). Comparison between numerical and analytical solutions for the receding contact problem, *Sigma Journal of Engineering and Natural Sciences, 2*, 333-346.

Yan J. & Mi C. (2017). Double contact analysis of multilayered elastic structures involving functionally graded materials, *Archieves of Mechanics, 69*(3), 199-221.

Yıldırım Ö., Pławiak P., Tan R.S. & Acharya U.R. (2018). Arrhythmia detection using deep convolutional neural network with long duration ECG signals, *Computers in Biology and Medicine, 102*, 411-420. https://doi.org/10.1016/j.compbiomed.2018.09.009